1992AJ....104.1533U

THE ASTRONOMICAL JOURNAL VOLUME 104, NUMBER 4 OCTOBER 1992

AN H I ABSORPTION LINE STUDY OF THE NONTHERMAL SHELL NEAR THE GALACTIC CENTER, G359.1−0.5 AND SEVERAL NEARBY UNUSUAL RADIO FEATURES

KEVEN UCHIDA AND MARK MORRIS

University of California-Los Angeles, Department of Astronomy, 8979 Math Sciences Building-156205, Los Angeles, California 90024

FARHAD YUSEF-ZADEH

Northwestern University, Department of Physics and Astronomy, Evanston, Illinois 60201

Received 1 May 1992; revised 19 June 1992

ABSTRACT

We present $\lambda 21$ cm spectral line observations, made with the C/D configuration of the VLA, of a remarkable Galactic center field containing: (1) G359.1−0.5, a complete nonthermal radio shell, (2) G359.2−0.8 (the "Mouse"), a nonthermal radio continuum feature with a cometary morphology, and (3) G359.1−0.2 (the "Snake"), a nonthermal object with a linear filamentary structure. Both G359.2−0.8 and G359.1−0.2 have been considered by some to be associated with the radio shell. The observations reveal that the nonthermal shell is surrounded by and is associated with atomic gas having large negative velocities (~ -75 to -190 km s^{-1}). Both the spatial distribution and velocity of the atomic gas are consistent with a previously reported complete ring of molecular material surrounding the nonthermal shell. Because of its apparent association with high velocity material, G359.1−0.5 is likely to be located at the distance of the Galactic center. The Snake also appears to be located near the Galactic center since both the 3 kpc arm and the -135 km s^{-1} feature (which is thought to be located within a few hundred parsecs of, and foreground to, the Galactic center) are clearly seen in absorption against this radio continuum source. The Mouse, however, appears to be a local object ($d \leqslant 5.5$ kpc) since neither of the H I features are seen in absorption against this source. Also revealed by this observation is a strong local radio continuum source (G359.28−0.26), located about 8′ from the edge of G359.1−0.5, with an apparent bow shock structure.

1. INTRODUCTION

G359.1−0.5 is a complete nonthermal shell of 12 arcminute radius located towards the Galactic center (Reich & Fürst 1984; Sofue *et al.* 1984). This object first came to our attention because it appears to be surrounded by a complete ring of high-velocity (-60 to -190 km s^{-1}), large-linewidth (35 to 50 km s^{-1}) molecular gas characteristic of that located near the Galactic center (Uchida *et al.* 1992, hereafter Paper I; Bally *et al.* 1988). The mass of the surrounding molecular material, determined from the observed ^{12}CO linewidth, is 2.5×10^6 $\mathcal{M}_\odot$. Based on this apparent association, we suggested in Paper I that G359.1−0.5 is an expanding bubble/superbubble, of 30 pc radius, which is sweeping up gas in the dense molecular environment of the Galactic center. If the nonthermal shell is indeed located at the distance to the Galactic center, then its age is limited to less than 2 Myr by the minimal extent of its sustained shear distortion (due to differential Galactic rotation).

Another interesting aspect of G359.1−0.5 is that it is centered on a field containing several unusual objects (Fig. 1), two of which have been speculated to be associated with the nonthermal shell. Located about 23 arcmin east of the shell's center is G359.2−0.8, a nonthermal feature known as the "Mouse" (Yusef-Zadeh & Bally 1987, 1989). The Mouse derives its name from its unusual morphology; it consists of a bright point source followed by a cometary tail that extends for about 10 arcmin toward the direction of the nonthermal shell. The spectral index of G359.2−0.8 ranges between +0.03 and −0.3, with the near-zero values being measured from its compact "head." Together with observed polarization values as high as 60% in the tail, these factors render it unlikely that G359.2−0.8 is an extragalactic head–tail source. G359.2−0.8 may instead be akin to a small group of Galactic objects believed to be compact sources, such as a neutron stars, which are traveling at a high velocities through the interstellar medium (Becker & Helfand 1985; Shaver *et al.* 1985). Indeed, Frail & Kulkarni (1991) have detected a 125 ms pulsar at the apex of one of these features (G5.4−1.2). These objects are associated with nearby supernova remnants, thus leading to speculation that they originated from an asymmetric supernova explosion or from the disruption of a centrally located binary system.

Crossing the northwestern perimeter (in celestial coordinates) of the nonthermal shell and extending nearly perpendicular to the Galactic plane for about 20 arcmin is G359.1−0.2, nicknamed the "Snake" (Gray *et al.* 1991; Yusef-Zadeh 1991). G359.1−0.2 is one of several nonthermal filamentary features that are found only within the inner degree of the Galactic center (Yusef-Zadeh *et al.* 1984; Morris & Yusef-Zadeh 1985; Bally & Yusef-Zadeh 1989; Bally *et al.* 1989; Yusef-Zadeh 1989); its spectral index, $\alpha = -0.5$, is typical of that measured from these filaments. One hypothesis is that these filaments are the

 0004-6256/92/101533-06$00.90 © 1992 Am. Astron. Soc. 1533

© American Astronomical Society • Provided by the NASA Astrophysics Data System

1992AJ....104.1533U

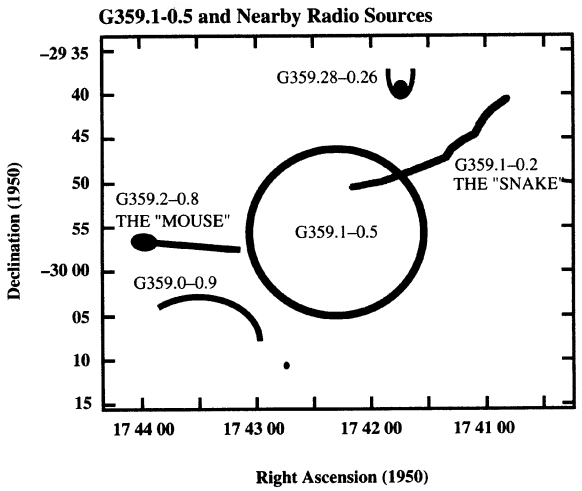

FIG. 1. Schematic diagram of G359.1−0.5 and surrounding features.

manifestations of current flows induced by high-velocity interactions between clouds and strong linear magnetic fields that are thought to exist within the Galactic center region (Sofue & Fujimoto 1987; Bally *et al.* 1988; Benford 1988; Morris & Yusef-Zadeh 1989). If G359.1−0.2 is indeed located at the distance of the Galactic center, then its overall length is 50 pc. G359.1−0.2 differs from the other nonthermal filaments because it is "kinked" at a few locations; the cause of this unusual behavior is not known.

In this paper we present the preliminary results of $\lambda 21$ cm VLA H I absorption observations and continuum images of G359.2−0.8, G359.1−0.2, and the nonthermal shell G359.1−0.5. This study was done in order to better constrain the distances to these features and thereby to help determine: (1) whether the nonthermal shell G359.1−0.5 is indeed associated with a surrounding ring of Galactic center molecular gas (Paper I), (2) whether G359.2−0.8, a possible runaway star, originated with the nonthermal shell, (3) whether G359.1−0.2, like the other filamentary structures, is located at the Galactic center, and (4) whether G359.1−0.2 is associated with the nonthermal shell. To date, the nonthermal shell and its interior region have been poorly characterized since past interferometric observations were centered on the Mouse and the Snake—both of which are strongly offset from the shell's center of symmetry. The observations done for this study were thus centered on the nonthermal shell to attain the first complete, high-resolution image of this feature and to detail any portions of the Mouse and the Snake that may fall on or within its perimeter.

2. OBSERVATIONS

The observations were done on 18 Feb 1991, between 14:00 and 21:00 LST, with the VLA in its hybrid C/D configuration. The data were taken in the 2AD spectral line mode with the central channel offset by -50 km s^{-1} with respect to the rest frequency of the $\lambda 21$ cm hyperfine transition. This negative velocity offset was done to ensure that all velocity components of the H I gas would be observed; negative velocities predominate at this Galactic longitude. The total bandwidth was 3.125 MHz corresponding to a velocity range of 660 km s^{-1}; 64 channels were used providing a velocity resolution of 10.3 km s^{-1}. The source 3C286(1328+307) ($S_{1.42}=14.85$ Jy) was observed as the primary flux calibrator and NRAO 530 (1730−130) ($S_{1.42}=16.05$ Jy) was used as the phase calibrator. Both NRAO 530 and 0134+329 were used in combination as bandpass calibrators. The pointing center of the observation is $\alpha_{1950}=17^h42^m15^s$, $\delta_{1950}=-29°56'00''$, the approximate center of the continuum shell G359.1−0.5.

The 21 cm channel and continuum images were produced and cleaned with the Astronomical Imaging Processing (AIPS) procedure MX. When a separate clean field was established around SgrA, a strong continuum source located 1° away at the Galactic center, MX was able to remove this feature's prominent sidelobes from each of the channel and continuum maps. The full images are 512 ×512 pixels in size, with a cellsize of 10 arcsec giving an angular coverage in the maps of 1°.42×1°.42, much larger then the primary beam size of an individual antenna (FWHM=34′). The synthesized beamwidth in the uniformly weighted images is 32.2×30.3 arcsec (P.A.= −56°.1) and in the naturally weighted maps is 55×45 arcsec (P.A.=−22°).

3. RESULTS AND DISCUSSION

3.1 Continuum Map

Figure 2 is a continuum image of the G359.1−0.5 region made from the channels free of apparent line emission ($-323<v<-230$ km s^{-1}, $161<v<233$ km s^{-1}); UVLIN was used to perform the selected channel integration in the UV domain. The image map was subsequently made with uniform UV visibility weighting. It has not been corrected for primary beam attenuation, which is substantial since the primary beam is smaller than the field shown. G359.1−0.5, located at map center, has a radius of about 12 arcmin or 30 pc if located at the distance of the Galactic center (assumed 8.5 kpc). The total flux density measured with the VLA, at 21 cm (1.42 Ghz), is 5.8 Jy. However, this value is only a lower limit because shell emission extended over more than 15′ is not sufficiently sampled in this observation. The fluxes reported by Reich & Fürst (1984), $S_{2.695}=10$ Jy and $S_{4.75}=8.1$ Jy, would appear to support this assertion if it is assumed that G359.1−0.5 maintains its nonthermal signature ($\alpha_{(2.695,4.75)}=-0.37$) near H I line frequencies.

The continuum image shows several noteworthy things: (1) The tail of G359.2−0.8 (the Mouse) extends only as far as the limb of the nonthermal shell, as appeared to be the case in the images of Yusef-Zadeh & Bally (1989), and does not appear to cross the shell itself. Running parallel to, and south of the Mouse is emission from G359.0−0.9, a partial nonthermal shell. (2) The Snake crosses the shell and extends for about 5 arcmin before terminating within the shell's interior at $\alpha_{1950}=17^h42^m15^s$, $\delta_{1950}=-29°52'$; it

© American Astronomical Society • Provided by the NASA Astrophysics Data System

1992AJ....104.1533U

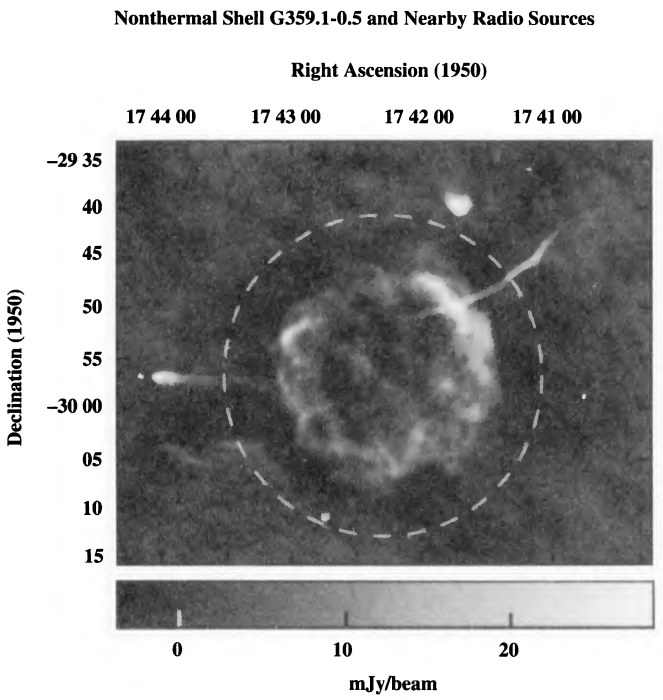

FIG. 2. Uniformly weighted $\lambda 21$ cm continuum map of G359.1−0.5 and surrounding features integrated between the velocities of $-323 < v < -230$ km s^{-1} and $161 < v < 233$ km s^{-1}. The dashed circle indicates the FWHM beamwidth.

does not appear to be an extension of the Mouse. The brightest portion of the continuum shell occurs along a ~5 arcmin segment where the radio filament G359.1−0.2 crosses its perimeter, perhaps an indication of an interaction between the two features.

Located northwest of the shell, at $\alpha_{1950} = 17^h41^m44^s$, $\delta_{1950} = -29°40'00''$, is G359.28−0.26, a strong continuum source with a bow shock morphology. Its axis of symmetry is aligned almost directly north–south. The total flux density of G359.28−0.26, measured within a 3.'2×3.'2 surrounding box, is 1.4 Jy. This object appears in the single-dish radio continuum surveys of the Galactic center, but the high-resolution image presented in Fig. 2 gives the first indication of its symmetric bow-shock morphology. Based on published survey fluxes (Reich & Fürst 1984, 2.695 and 4.750 GHz; Altenhoff *et al.* 1978, 4.875 GHz; Sofue *et al.* 1984, 10.5 GHz), the spectrum of this source has a turnover frequency, indicating $\tau = 1$, near 1.3 GHz. The electron density, n_e, of this bow-shock H II region is thus $2 \times 10^3 L^{-0.5}$ cm^{-3}, where L is its diameter in parsecs.

3.2 H I Emission/Absorption Maps of the G359.1−0.5 Region

Figure 3(a) is a map of H I with velocities integrated between −75 and −190 km s^{-1}. The UV visibilities were naturally weighted in order to *maximize* the sampling of extended line emission. Superimposed on this image is a contour map of the continuum emission from G359.1−0.5. This comparison shows that strong 21 cm absorption (dark regions) is correlated with the continuum emission. It also reveals high negative-velocity H I gas

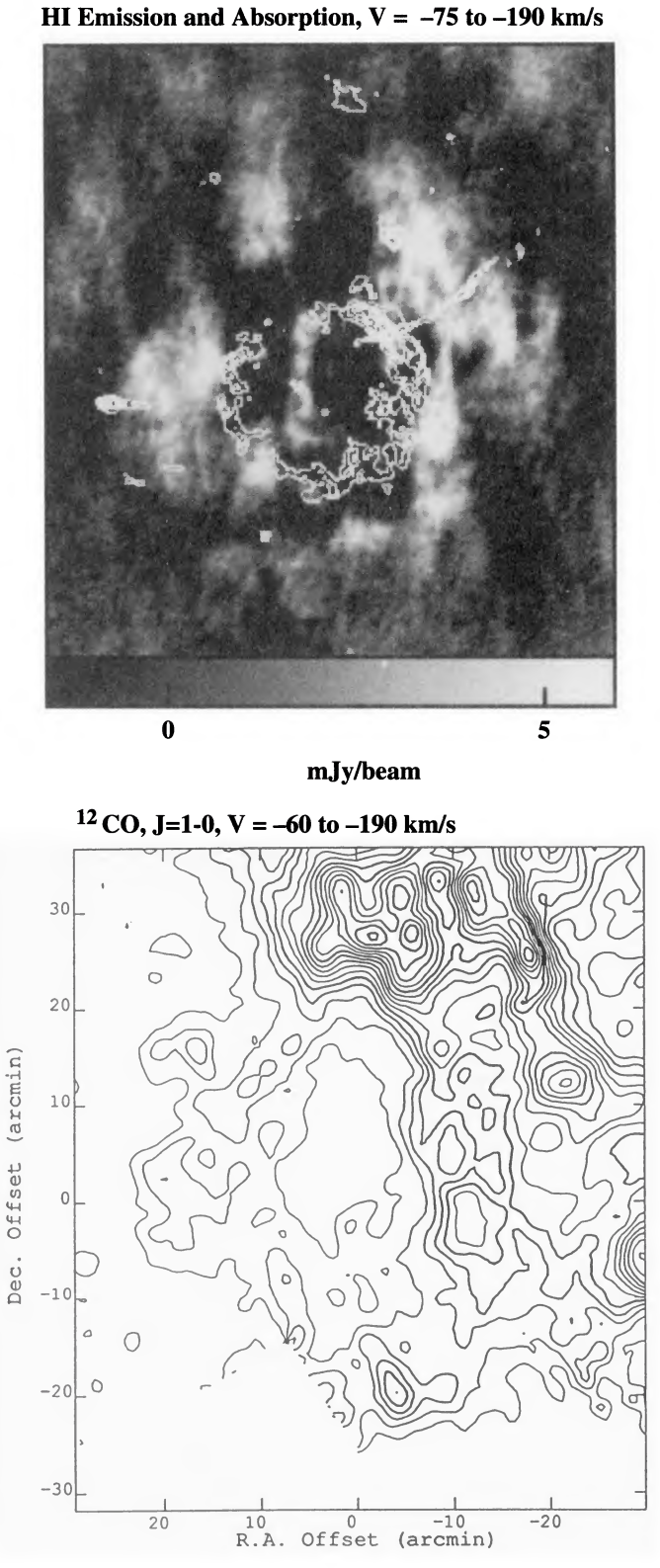

FIG. 3. Top: Naturally weighted map showing H I emission, integrated between $-190 < V < -75$ km s^{-1}, surrounding the radio continuum shell. This image has not been corrected for primary beam attenuation. The "ring" of H I emission, however, remains prominent even after the proper correction is performed. Superimposed on this image is a 21 cm continuum contour map (in white) of G359.1−0.5. Bottom: Contour map of ^{12}CO $J = 1-0$ emission, in the same velocity range, surrounding the nonthermal shell. The observations are part of the survey of the Galactic center made with the 7 m offset Cassegrain telescope at the AT&T Bell Laboratories on Crawford Hill, New Jersey (Bally *et al.*, in preparation). The contour levels are in intervals of 45 K km s^{-1}.

© American Astronomical Society • Provided by the NASA Astrophysics Data System

1992AJ....104.1533U

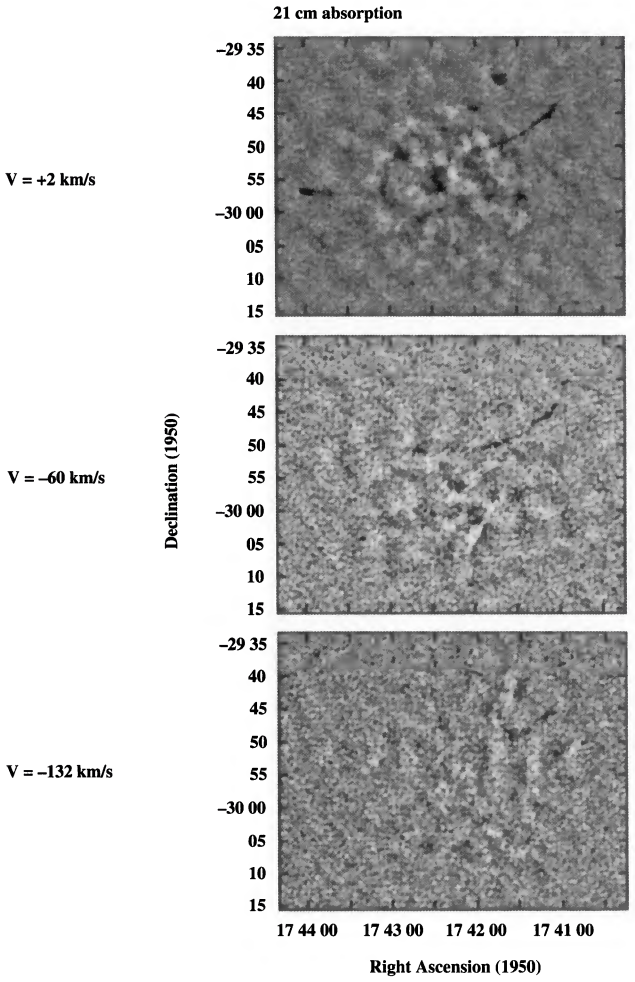

FIG. 4. λ21 cm absorption maps integrated over 10 km s^{-1} velocity intervals and centered on $V=+2$ km s^{-1} (top), -60 km s^{-1} (center), and -132 km s^{-1} (bottom). All frames have the same spatial scale. The center and bottom panels are at the approximate velocities of the 3 kpc arm and the "-135 km s^{-1} feature," respectively. The transfer function of each image was independently adjusted to maximize the absorption regions. Visibilities corresponding to UV spacings <0.5 kλ were excluded when producing these maps.

(in emission) surrounding the nonthermal shell; the concentricity of the continuum and line emission is striking. On the large scale, both the strongest line and continuum emission is observed from the eastern and western portions of the shell. The H I line emission corresponds closely both in velocity and spatial distribution to the ^{12}CO emission observed surrounding the shell (Uchida *et al.* 1992). Figure 3(b) is a contour map of ^{12}CO emission from the Bell Labs survey of the Galactic center. The molecular gas displays linewidths between 35 and 50 km s^{-1} and is typical of that seen in Galactic center clouds. The distribution of the observed H I emission supports our assertions in Paper I that the nonthermal shell is associated with the high-velocity, large-linewidth gas and is thus located at the Galactic center.

Figures 4(a), 4(b), and 4(c) show H I channel maps that are integrated over $\sim$10 km s^{-1} velocity intervals and centered on $+2$, -60, and -132 km s^{-1}, respectively. These maps were made excluding visibilities corresponding to baseline separations of less than 0.5 kλ in order to minimize the contaminating extended emission. A velocity of -60 km s^{-1} corresponds approximately to that of the 3 kpc arm which, at the longitude of our map ($l\cong 359°$), has a latitude extent of $-1°.5 \leqslant b \leqslant 1°$ (Fig. 14 of Burton *et al.* 1977). The -132 km s^{-1} window incorporates the velocity range of the "-135 km s^{-1} feature" (Robinson & McGee 1970; Cohen 1977). The precise distance to the -135 km s^{-1} feature is not well established, but it is likely to be foreground to most of the Galactic center continuum emission because it is seen in OH absorption. Whether it is part of the approaching portion of expanding molecular ring (EMR: Scoville 1972; Kaifu *et al.* 1972; Bania 1977; Güsten & Downes 1980), or whether it is the kinematical response to a strong bar potential in the nucleus (Binney *et al.* 1991), it is, in either case, situated within a few hundred parsecs of the Galactic center. Regardless, it is believed to be much closer to the Galactic center than the 3 kpc arm. Position–velocity maps from the Bell Labs ^{12}CO survey of the Galactic center (Bally *et al.* 1992, in preparation) indicate that the -135 km s^{-1} feature extends out to $b \cong -0°.6$ at the longitude of the nonthermal shell. At high positive velocities is the "expanding arm at $+135$ km s^{-1}" (Rougoor 1964; van der Kruit 1970; Cohen 1975). This large-scale feature extends for nearly 30° in longitude and, at $l=359°$, spans about 3° in latitude ($-1° \leqslant b \leqslant 2°$). It is thought to be located about 2 kpc *behind* the Galactic center.

The $+2$ km s^{-1} map serves to locate the small-scale radio continuum objects in this region. The local gas in the $+2$ km s^{-1} frame is seen in absorption against all of the radio continuum features in our map—except for the nonthermal shell which, because of its extended structure, has been resolved out of these maps (in which visibilities from UV pairs <0.5 kλ are excluded). Because the continuum emission intensity varies slowly over the extent of the shell and because it is very weak at some locations, the shell is not very well defined in absorption, even in the uniformly weighted images (which include all visibilities). In the following section we present spectra integrated over various subsections of the shell that better illustrate its absorption characteristics.

The 3 kpc arm at -60 km s^{-1} and the -135 km s^{-1} feature appear clearly in absorption against G359.1$-$0.2 (the Snake). However, no evidence of absorption can be seen at either of these velocities toward G359.2$-$0.8 (the Mouse) or G359.28$-$0.26 (the H II region) in spite of the fact that both have peak continuum brightness temperatures (T_b=226 and 208 K, respectively) that are significantly greater than that of the Snake (T_b=40 K). Because the Mouse is located relatively far from the Galactic plane ($b=-0°.8$), it may be beyond the latitudinal extent of the -135 km s^{-1} feature ($-0°.6 < b < 0°$); however, it is still well within the latitudinal bounds of the 3 kpc arm ($-1°.5 < b < 1°$). Although it is not shown here, the "expanding arm at $+135$ km s^{-1}," located behind the Galactic center, does not appear in absorption against any of these features. Moreover, absorption is not apparent in *any* of the high positive velocity frames ($v > 30$ km s^{-1}). The absorption

© American Astronomical Society • Provided by the NASA Astrophysics Data System

1992AJ....104.1533U

maps thus indicate that G359.2−0.8 (the Mouse) and the H II region G359.28−0.26 are local objects that are foreground to the 3 kpc arm. On the other hand, both G359.1−0.2 (the Snake) and the nonthermal shell (G359.1−0.5) are constrained to a distance of $8 < d < 10.5$ kpc, for a Galactic center distance of 8.5 kpc. Using the Σ–D relationship, Sofue *et al.* (1984) determined that G359.1−0.5 is located at a distance of 6.5 kpc. Our results appear to be in agreement given the uncertainties in both the Σ–D relationship and the estimated distance of the Galactic center.

3.3 Absorption Spectra

Figure 5 displays absorption spectra integrated over selected regions (shown in the accompanying inverse greyscale image) of a datacube produced by uniform weighting with no UV restrictions. The two vertical dashed lines in each frame indicate velocities of −60 and −135 km s^{-1}. The region-averaged absolute continuum level is indicated (in mJy/beam) to the right of each spectrum. These levels may be underestimated (e.g., for spectra 3 and 10) since some of the extended continuum emission is being resolved out of the images.

Spectra 1, 4, and 5, of the Mouse, the H II region, and the Snake, respectively, show absorption (or the lack of it) consistent with that seen in the two-dimensional maps. For example, spectrum 1 (of the Mouse) shows no more absorption at −60 km s^{-1} than do spectra 2 and 3 of nearby background regions. Spectrum 5 (of the Snake) shows strong absorption by the 3 kpc arm and the −135 km s^{-1} feature with maximum line depths of $\tau_{60}=1.1$ and $\tau_{135}=0.3$, respectively. Spectra 6, 7, 8, and 9 support the hypothesis that the nonthermal shell is located near the Galactic center. Spectrum 6, which is integrated over the eastern hemisphere of the shell to avoid inclusion of the Snake, shows absorption from both H I features. Absorption toward region 7 is more pronounced yet (τ_{60} and $\tau_{135}=0.3$). Spectrum 8 (from the brightest portion of the continuum shell) displays absorption features, although not as prominently as might be expected. Here, the interpretation of the spectrum is complicated because strong emission from the surrounding ring of H I gas may be superimposed on the absorption features. The spectrum from region 9, part of the western portion of the shell, exhibits absorption line depths of $\tau_{60}=0.1$ and $\tau_{135}=0.2$.

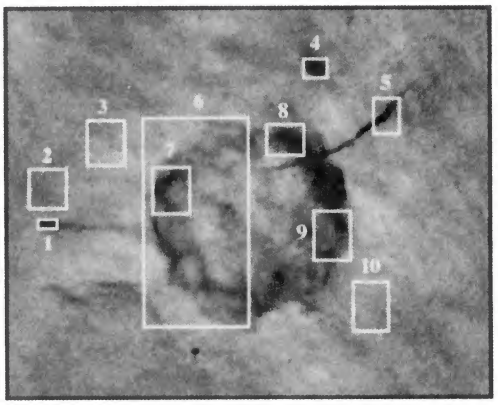

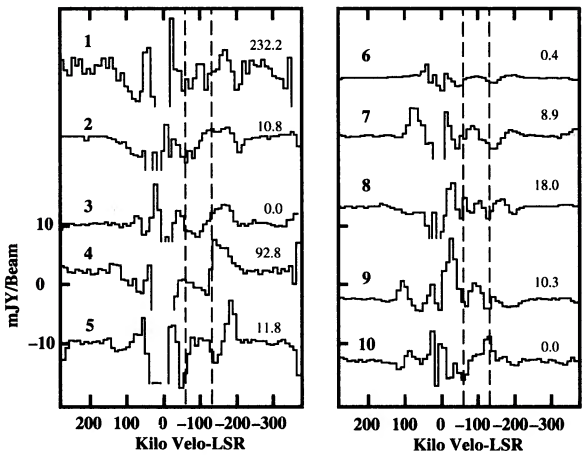

FIG. 5. Integrated H I spectra, from the regions indicated in the reverse grayscale continuum image, produced from a naturally weighted datacube; all spectra are of the same vertical scale. The region-averaged absolute continuum level (in mJy/beam) is indicated to the right of each spectrum. Because the incomplete sampling leads to an artificial ring of negative flux values surrounding the shell (the darkest areas of Fig. 2), the mean continuum level in some boxes (particularly box 6) is consequently depressed.

3.4 HI Optical Depths and Column Densities

Table 1 presents H I opacity and column density determinations of the local foreground H I component (+27 to −14 km s^{-1}), the 3 kpc arm (−35 to −76 km s^{-1}) and the "−135 km s^{-1}" feature (−117 to −168 km s^{-1}) toward three of the observed continuum sources. These velocity limits were determined by inspection of the absorp-

TABLE 1. H I optical depths and column densities toward G359.2−0.8, G359.1−0.2, and G359.28−0.26.

	G359.2−0.8 The Mouse	G359.1−0.2 The Snake	G359.28−0.26 H II region
τ (+27 to −14 km s^{-1})	0.7	1.4	1.8
τ (−35 to −76 km s^{-1})	...	0.3	...
τ (−117 to −168 km s^{-1})	...	0.3	...
N(H) (+27 to −14 km s^{-1}) (cm^{-2})	5.3 $T_s\times10^{21}$	1.1 $T_s\times10^{22}$	1.4 $T_s\times10^{22}$
N(H) (−35 to −76 km s^{-1})	...	2.3 $T_s\times10^{21}$	...
N(H) (−117 to −168 km s^{-1})	...	2.8 $T_s\times10^{21}$	...

© American Astronomical Society • Provided by the NASA Astrophysics Data System

1992AJ....104.1533U

tion spectra toward the continuum sources. An H I opacity map was made following the methods of Lasenby *et al.* (1989) and by assuming the H I spin temperature of the absorbing foreground gas to be zero ($T_s=0$). The use of nonzero values of T_s resulted in unrealistic values of τ (either negative or undefined)—this may be explained if much of the extended foreground H I emission has been resolved out of the line maps. The τ values presented in the table are averages taken over the entire extent of the continuum sources or, for the Snake, over portions located outside of the nonthermal shell. The actual spin temperature, T_s, of either of the H I features or of the near-zero velocity H I component is not well known and is likely to vary across the mapped region; it is thus left as a variable in the H I column density results presented in the table.

The nature of the H I absorption and the presence of H I emission toward the nonthermal shell complicates the opacity and column density determination for its surrounding gas. The continuum emission from the nonthermal shell is relatively weak ($T_b \leqslant 24$ K) and extended and varies considerably in intensity. A proper column density estimate of the material surrounding the ring thus requires a more thorough analysis than that done here and will be reserved for a future paper.

4. CONCLUSIONS

The observations presented here leave open the possibility that the Snake and the nonthermal shell are associated. While the approaching portion of the EMR (the -135 km s^{-1} feature) is seen in absorption against both these features, the expanding arm at $+135$ km s^{-1} is not; the distances to both these objects are thus constrained to within $8 < d < 10.5$ kpc. If the Snake is akin to other filamentary structures seen only near the Galactic center, then this provides further evidence that it lies within a few hundred parsecs of the Galactic center. The nonthermal shell is brightest along a segment where it intersects the Snake, a possible result of energy transfer between the two. Additional high resolution observations of the region of intersection are needed to uncover and to detail any small scale manifestations of an association.

The low-resolution images show that the nonthermal radio continuum shell is surrounded by high-velocity H I gas and that there is a strong anticorrelation between the continuum shell brightness and the intensity of the H I emission from nearby portions of the surrounding shell. The H I emission, in turn, corresponds both in velocity and spatial extent to a massive and complete ring of Galactic center molecular material surrounding the nonthermal shell. Together with the distance determined for the shell, these findings support our claim that the nonthermal shell is associated with the molecular ring located near the Galactic center. If this is indeed so, the energies needed to have cleared the surrounding gas, and the physical size of the nonthermal shell ($r=30$ pc) require that it have originated from multiple supernova explosions rather than from a single event. G359.1−0.5 (the nonthermal shell) may thus be the best example to date of the interaction between an expanding supernova-generated shell and a surrounding atomic/molecular cloud. The molecular data are discussed in detail and a dynamical model of the shell expansion is presented in Paper I.

Unless the Mouse (G359.2−0.8) happens to coincidentally lie in a hole in the 3 kpc arm gas, it must be regarded as a foreground object lying between the Sun and the 3 kpc arm. The hypothesis that it is associated with the nonthermal shell G359.1−0.5 is no longer attractive. This new finding rekindles the question of the origin of the Mouse, which is now more challenging since the only obvious candidate in this region now seems unlikely.

REFERENCES

Altenhoff, W. J., Downes, D., Pauls, T., & Schraml, J. 1978, A&AS, 35, 23
Bally, J., Stark, A. A., Wilson, R. W., & Henkel, C. 1988, ApJ, 324, 223
Bally, J., Yusef-Zadeh, F., & Hollis, J. M. 1989 in IAU Symp. 136: The Center of the Galaxy, ed. M. Morris (Dordrecht: Kluwer), p. 189
Bally, J., & Yusef-Zadeh, F., 1989, ApJ, 336, 173
Bania, T. M. 1977, ApJ, 216, 381
Becker, R. H., & Helfand, D. J. 1985, Nature, 313, 115
Benford, G. 1988, ApJ, 333, 735
Binney, J., Gerhard, O. E. Stark, A. A., Bally, J., & Uchida, K. 1991 MNRAS, 252, 210
Burton, W. B., Gallagher, J. S., & McGrath, M. A. 1977, A&AS, 29, 123
Cohen, R. J. 1975, MNRAS, 171, 659
Cohen, R. J. 1977, MNRAS, 178, 547
Frail, D. A., & Kulkarni, S. R. 199, Nature, 352, 785
Gray, A. D., Cram, L. E., Ekers, R. D., & Goss, W. M. 1991, Nature, 353, 237
Güsten R., & Downes, D. 1980, A&A, 87, 6
Kaifu, N., Kato, T., & Iguchi, T. 1972, Nature Phys. Sci., 238, 105
Lasenby, J., Lasenby, A. N., & Yusef-Zadeh, F. 1989, ApJ, 343, 177
Morris, M., & Yusef-Zadeh, F. 1985, AJ, 90, 2511
Morris, M., & Yusef-Zadeh, F. 1989, ApJ, 343, 703
Reich, W., & Fürst, E. 1984, A&AS, 57, 165
Robinson, B. J., & McGee, R. X. 1970, AuJPh, 23, 405
Rougoor, G. W. 1964, Bull. Astron. Inst. Neth., 17, 381
Sanders, R. H., & Wrixon, G. T. 1974, A & A, 33, 9
Scoville, N. Z. 1972, ApJ, 175, L127
Shaver, P. A., Salter, C. J., Patniak, A. R., van Gorkom, J. M., & Hunt, G. C. 1985, Nature, 313, 113
Sofue, Y., & Fujimoto, M. 1987, ApJ, 319, L73
Sofue, Y., Handa T., Nakai, N., Hirabayashi, H., Inoue, M., & Akabane, K. 1984, PASJ (submitted)
Uchida, K. I., Morris, M., Bally, J., Pound, M., & Yusef-Zadeh, F. 1992, ApJ, (in press) (Paper I)
van der Kruit, P. C. 1970, A&A, 4, 462
Yusef-Zadeh, F. 1989, in The Center of the Galaxy, IAU Symposium No. 136; edited by M. Morris (Kluwer, Dordrecht), p. 243
Yusef-Zadeh, F., 1991 Highlights of Astronomy, Vol. 9, edited by J. Bergeron, (Kluwer, Dordrecht) (in press)
Yusef-Zadeh, F., & Bally, J. 1987, Nature, 330, 455
Yusef-Zadeh, F., & Bally, J. 1989 in The Center of the Galaxy, IAU Symposium No. 136, edited by M. Morris (Kluwer, Dordrecht), p. 197
Yusef-Zadeh, F., Morris, M., & Chance, D. 1984, Nature, 310, 557

© American Astronomical Society • Provided by the NASA Astrophysics Data System